NIH Public Access
Author Manuscript
Exp Cell Res. Author manuscript; available in PMC 2011 February 1.

Published in final edited form as:
Exp Cell Res. 2010 February 1; 316(3): 452–465. doi:10.1016/j.yexcr.2009.09.020.

SAM Pointed Domain ETS Factor (SPDEF) regulates terminal differentiation and maturation of intestinal goblet cells

Taeko K. Noah[1], **Avedis Kazanjian**[1], **Jeffrey Whitsett**[2,3], and **Noah F. Shroyer**[1,2]

[1]Division of Gastroenterology, Hepatology & Nutrition, Cincinnati Children's Hospital Medical Center and University of Cincinnati College of Medicine, Cincinnati, Ohio, USA.

[2]Division of Developmental Biology, Cincinnati Children's Hospital Medical Center and University of Cincinnati College of Medicine, Cincinnati, Ohio, USA.

[3]Division of Pulmonary Biology, Cincinnati Children's Hospital Medical Center and University of Cincinnati College of Medicine, Cincinnati, Ohio, USA.

Abstract

Background & Aims: SPDEF (also termed PDEF or PSE), is an ETS family transcription factor that regulates gene expression in the prostate and goblet cell hyperplasia in the lung. *Spdef* has been reported to be expressed in the intestine. In this paper, we identify an important role for Spdef in regulating intestinal epithelial cell homeostasis and differentiation.

Methods: SPDEF expression was inhibited in colon cancer cells to determine its ability to control goblet cell gene activation. The effects of transgenic expression of Spdef on intestinal differentiation and homeostasis were determined.

Results: In LS174T colon cancer cells treated with Notch/γ-secretase inhibitor to activate goblet cell gene expression, shRNAs that inhibited *SPDEF* also repressed expression of goblet cell genes *AGR2*, *MUC2*, *RETLNB*, and *SPINK4*. Transgenic expression of Spdef caused the expansion of intestinal goblet cells and corresponding reduction in Paneth, enteroendocrine, and absorptive enterocytes. Spdef inhibited proliferation of intestinal crypt cells without induction of apoptosis. Prolonged expression of the Spdef transgene caused a progressive reduction in the number of crypts that expressed Spdef, consistent with its inhibitory effects on cell proliferation.

Conclusions: Spdef was sufficient to inhibit proliferation of intestinal progenitors and induce differentiation into goblet cells; SPDEF was required for activation of goblet cell associated genes *in vitro*. These data support a model in which Spdef promotes terminal differentiation into goblet cells of a common goblet/Paneth progenitor.

Introduction

The intestinal epithelium is dynamically regulated to continuously produce a diversity of cell types throughout life. Notch signaling has been shown to control cell fate determination and self renewal of intestinal stem cells [1-3], wherein active Notch is required for stem cell self-renewal and absorptive enterocyte differentiation. Atoh1, a target of Notch repression via Hes1, is required for secretory (goblet, Paneth, and enteroendocrine) cell formation [4].

Correspondence: Noah F. Shroyer, Ph.D. Division of Gastroenterology Cincinnati Children's Hospital MLC 2010 3333 Burnet Avenue Cincinnati, OH 45229 noah.shroyer@cchmc.org Office: 513-636-0129 Fax: 513-636-5581 Lab: 513-636-4081.
Author Contributions: TKN, JW, and NFS conceived and designed the study; TKN, AK, and NFS performed the study; all authors interpreted the results; TKN and NFS wrote the manuscript; NFS supervised and obtained funding for the study.

Financial Disclosure: The authors have no disclosures to report.

NIH-PA Author Manuscript
NIH-PA Author Manuscript
NIH-PA Author Manuscript

NIH-PA Author Manuscript

NIH-PA Author Manuscript

NIH-PA Author Manuscript

A model has developed in which a balance between Hes1 and Atoh1 expression—controlled by Notch activity—determines absorptive vs. secretory cell differentiation. Analyses of Ngn3 showed its essential role in differentiation of enteroendocrine cells, and also supported the concept of an Atoh1-dependent common secretory progenitor that can select among multiple secretory cell fates [5-7]. Our studies further supported this model by demonstrating that Gfi1 functions downstream of Atoh1 to select enteroendocrine versus Paneth/goblet cell fates [8].

The differentiation and maturation of Paneth and goblet cells is controlled by several genes. The Wnt/β-catenin pathway is essential for proliferation and differentiation of all intestinal epithelial cells, especially Paneth cells [9-13]. Recently, Lkb1 was shown to negatively regulate goblet and Paneth cell differentiation, potentially via the Notch pathway [14]. Additional genes, including Elf3, Klf4, Klf9, and Sox9 are essential for normal differentiation of multiple intestinal epithelial cell types [15-19]. However, no factor has been identified that positively regulates differentiation of goblet and Paneth cells from their common progenitors. Recently, we found that *Spdef* mRNA expression was reduced in *Atoh1* and *Gfi1* mutant intestines, suggesting its potential role in goblet and/or Paneth cell differentiation [8,20].

SPDEF (also called PDEF or PSE) was first described as a prostate-specific ETS transcription factor, at which time intestinal expression was noted [21,22]. In the prostate, SPDEF interacts with NKX3.1 and the androgen receptor to regulate prostate-specific antigen expression [21,23]. SPDEF forms a unique subfamily among the 27 mammalian Ets factors [24], which is reflected in its preference for binding DNA elements with a GGAT core sequence rather than the Ets-family consensus GGAA [21,25]. SPDEF is present in prostate and breast epithelium and its expression is reduced in prostate and breast cancers [26], where it is thought to have a potential tumor suppressor function by inhibiting cell migration and invasion [22,27,28]. Recently, we showed a role for SPDEF in regulating goblet cell hyperplasia in the lung, where it interacts with NKX2.1 (TTF-1) to influence target gene expression [29]. A role for SPDEF in the regulation of intestinal epithelial differentiation has not been described. Here, we test the hypothesis that SPDEF directs differentiation of goblet cells from fate-restricted secretory progenitors specified by Atoh1 and Gfi1.

Materials and Methods

Animals and treatment

Spdef$^{dox\text{-}intestine}$ mice [*Fabp-cre; Rosa-rtta; TRE2-Spdef*] were generated by crossing *Rosa26-lox-STOP-lox-rtta-IRES-EGFP* (*Rosa-rtta*) [30] mice purchased from the Jackson Laboratory, with *Fabp-cre* mice [31] and *TRE2-Spdef* mice [29]. *Spdef*$^{dox\text{-}intestine}$ mice were genotyped as previously described [29-31]. A separate cohort of mice was generated using a pan-intestinal cre driver [*Villin-cre; Rosa-rtta; TRE2-Spdef*]. Four-week-old mice were fed chow containing doxycycline (DOX) for 2, 6 or 60 days. The mice were injected with 50mg/kg bromodeoxyuridine (BrdU) 2 hours prior to sacrifice. Mice were housed in microisolator cages in a pathogen free environment with sterilized food, water and bedding, in accordance with the Cincinnati Children's Hospital Institutional Animal Care and Use Committee.

Tissue preparation

Intestines were dissected and flushed with ice-cold phosphate buffered saline (PBS). A segment of the intestines was flushed and embedded in cold optimum cutting temperature embedding medium (OCT), then frozen on dry ice. Another segment of the intestines was fixed in 4% paraformaldehyde in PBS (PFA) overnight, transferred to 70% ethanol, then

NIH-PA Author Manuscript

NIH-PA Author Manuscript

NIH-PA Author Manuscript

processed and imbedded in paraffin. Sections (5 μm) were cut for paraffin and OCT embedded tissues. Paraffin embedded sections were deparaffinized and rehydrated, OCT embedded sections were fixed in 4% PFA for 15 min before staining. Tissues from *Atoh1*$^{\Delta intestine}$, *Gfi1*$^{-/-}$, and control littermate mice were obtained as archival samples from our previously published studies [8,32].

Histology, Immunohistochemistry and In situ hybridyzation

Antibodies and concentrations used were: anti-BrdU at 1:100 (G3G4, Developmental Studies Hybridoma Bank-DSHB); anti-chromogranin A at 1:1000 (ImmunoStar, Inc. #20085-112031); anti-Ki67 at 1:1000 (Novacastra Laboratories Ltd., #NCL-Ki67P); anti-DPPIV at 1:100 (R&D systems, Inc., #AF954); anti-lysozyme at 1:1000 (Zymed Laboratories, Inc., #18-0039); anti-Spdef at 1:500 for immunofluorescent/1:5000 for immunohistochemistroy [29]; anti-MUC2 at 1:100 (Santa cruz, #H-300); Ulex europus agluttinin 1 (UEA1) conjugated to fluoresceine (FITC) at 50 μg/ml (Sigma, #L9006); Phalloidin conjugated to FITC at 1:100 (Sigm, #P5282a). Antigen retrieval was performed in tris-EDTA buffer (10mM tris, 1mM EDTA, 0.05% tween 20, pH9.0) using a microwave for 4 min at full power and twice for 5 min at 50% power. Immunohistochemistry was performed as previously described [32] with a modification in antigen retrieval buffer. Vectastain ABC kits along with the diaminobenzidine peroxidase substrate kit (Vector laboratories) were used to visualize the staining. For immunofluorescent analysis, sections were incubated for 1 hour at room temperature in 4% normal serum in PBS. Primary antibodies against Spdef and lysozyme, Muc2, DPPIV, Ki67 or chromogranin A were co-incubated on the sections in blocking solution (4% normal goat serum in PBS) overnight at 4°C. Slides were rinsed in PBS, then incubated in goat anti-rabbit-Alexa 488 and goat anti-guinea pig Alexa 594 (Invitrogen) secondary antibodies, each at 1:200, in blocking solution. Slides were washed in PBS, and mounted in VectaShield hard set with DAPI (Vector laboratories, Inc.). For double staining with UEA1 or Phalloidin and Spdef, tissues were incubated sequentially, first with UEA1 or Phalloidin, then with Spdef antibody followed by the secondary antibody incubation. For double staining with BrdU and Spdef, sections were incubated first with the Spdef antibody, then with 2M HCl for 20 min followed by 2 min incubation with 0.1M sodium borate pH 8.5, followed by the BrdU antibody. For the detection of BrdU, endogenous immunoglobulins were blocked and primary and secondary antibody incubations were performed using the M.O.M. kit following the manufacturer's recommendations (Vector Laboratories). In situ hybridization was performed as previously described [32]. The number of Spdef-expressing and the total number of crypts in *Spdef*$^{dox\text{-}intestine}$ were counted in ileum of 2 day, 6 day and 2 month DOX treated mice. The percent of BrdU-positive cells in wild type and *Spdef*$^{dox\text{-}intestine}$ crypts was determined for each animal. The number of chromogranin A positive cells was determined in wild type and *Spdef*$^{dox\text{-}intestine}$ villi. ANOVA was performed to measure significance.

Transmission Electron Microscopy

Ilea were dissected, flushed with cold-PBS, fixed in 3% glutaraldehyde/0.175M cacodylate buffer followed by postfix in 1% osmium tetroxide/0.175M cacodeylate buffer, dehydrated and embedded in LX-112 resin. Serial thick sections and thin sections were obtained. The resin of thick sections was removed by immersing the sections in aged 3% sodium hydroxide in absolute ethanol for 20 min, followed by four times of 5 min wash in absolute ethanol. These sections were immunologically stained for lysozyme as above at an antibody dilution of 1:100, then conterstained with PAS. Thin sections were stained with uranyl acetate and lead citrate, and analyzed with Hitachi H7600.

NIH-PA Author Manuscript

NIH-PA Author Manuscript

NIH-PA Author Manuscript

Cecum lysate preparations and immunoblotting

Lysates were extracted from cecal tissues from wild-type and *Spdef*$^{dox\text{-}intestine}$ mice homogenized in lysis buffer (1× Phosphate Buffered Saline, 1% NP-40, 0.5% sodium deoxycholate, 0.1% SDS, 0.7 mM EDTA supplemented with protease and phosphatase inhibitors). Antibodies used for immunoblot analysis: anti-Spdef at 1:2000 [29]; anti-actin mouse IgM (1:100, JLA20; DSHB); anti-Relm-β (1:1000, a gift from Dr. Gary Wu, University of Pennsylvania). The membranes were incubated with horseradish peroxide (HRP)-conjugated secondary antibodies (1:5000, Jackson Immunoresearch Laboratories, Inc.). Band density was measure with ImageJ software. The signal for the protein of interest was standardized to its respective actin loading control.

Cell culture, treatments and lentiviral vectors

LS174T cell line was cultured in MEM medium supplemented with 10% fetal calf serum (Perbio). All culture experiments were done at 37 °C in 5% CO_2. Cells were transduced with recombinant lentivirus carrying SPDEF 548 shRNA, SPDEF 550 shRNA or non-targeting control 24 hours after cell passage. Forty-eight hours after transduction, cells were treated with 5 μM DAPT (Sigma) reconstituted in dimethylsulfoxide (DMSO) or DMSO alone for 4 days, with the media changed daily. Vesicular stomatitis virus-G pseudotyped lentivirus carrying shRNA plasmids targeting SPDEF (Sigma MISSION shRNA: TRCN0000016550 (SPDEF 550), TRCN0000016548 (SPDEF 548)) or non-targeting control (Sigma MISSION shRNA: SHC002) were generated by Viral core facility at Cincinnati Children's Hospital Medical Center.

Quantitative reverse-transcriptase polymerase chain reaction (RT-qPCR)

RNA was purified from the small and large intestine isolated from wild-type and *Spdef*$^{dox\text{-}intestine}$ mice using Trizol (Invitrogen) according to the manufacturer's recommendations. Trizol-purified RNA (100 μg) was subjected to DNase digestion and further purification (RNeasy Mini; Qiagen); 2 μg of total RNA was reverse transcribed (Superscript III, Invitrogen), and cDNA equivalent to 100 ng of RNA used for SYBR Green–based real-time PCR using an Mx3005 (Stratagene). Small and large intestine RNA from wild-type and *Spdef*$^{dox\text{-}intestine}$ mice was compared using the standard curve method of relative quantification. Gene expression levels were normalized to the expression of GAPDH. For cell culture, cells were harvested by directly adding RNA lysis buffer provided in Rneasy Mini Kit (Quiagen) after rinsing with PBS twice. RNA was purified using the kit according to the manufacture's recommendations. In column DNA digestion step was performed as the manufacture's recommendation. cDNA was synthesized and analyzed as described above. Primer sequences were GAPDH, 5′-AATGAAGGGGTCATTGATGG -3′ and 5′-AAGGTGAAGGTCGGAGTCAA ; SPDEF, 5′-GGGGATACGCTGCTCAGAC -3′ and 5′-GCACTGCAGCAGACAGCTC -3′; AGR2, 5′-CGACTCACACAAGGCAGGT -3′ and 5′-TTTTTGGCTCCAGGTTTGAC -3′; SPINK4, 5′-CAGGAAAGCTCCCTTTCTCAA -3′ and 5′-AAGCAGAGCTGGCATTCATT -3′; MUC2, 5′-TGTAGGCATCGCTCTTCTCA-3′ and 5′-GACACCATCTACCTCACCCG -3′; RETLNB, 5′-AGTGTCAAAAGCCAAGGCAG -3′ and 5′-AGTGGTCCAGTCCACCACAC-3.

Results

Cellular localization of Spdef in gastrointestinal epithelium

We determined the expression pattern of Spdef in the small intestine and colon using immunohistochemistry and immunofluorescent staining. Shown in Figure 1, intense nuclear staining of Spdef was observed in a subset of progenitor cells within the crypts, as well as goblet cells marked by Alcian blue in both crypts and villi. Dual immunofluorescence

NIH-PA Author Manuscript

NIH-PA Author Manuscript

NIH-PA Author Manuscript

labeling showed no overlap between Spdef and enteroendocrine cells (marked with chromogranin A, Figure 1D). Spdef stained a subset of Paneth cells (marked with lysozyme, Figure 1E and shown by the white arrow in 1B). The majority of Spdef-expressing cells in both small intestine and colon were negative for the proliferation marker Ki67 (Figure 1F) In the duodenum, intense Spdef staining of the submucosal Brunner's gland was observed (Supplemental Figure 1A). Spdef staining was detected in the glands of the stomach (Supplemental Figure 1B-C). Together, these data show that Spdef is expressed in a subset of gastrointestinal progenitor and secretory cells.

Spdef expression is dependent on Atoh1 and Gfi1

Our previous studies showed a decrease in Spdef mRNA expression in crypts lacking Atoh1 and Gfi1 [8,20]. To elucidate the hierarchy of Atoh1, Gfi1, and Spdef, we examined Spdef expression in Atoh1- and Gfi1-null tissues. We found that Spdef is absent from *Atoh1*-null crypts that lack all intestinal secretory cells [32] (Figure 2A-B), and is quantitatively reduced in *Gfi1*-null crypts that have few goblet and no Paneth cells (Figure 2C-D). These data suggest that Spdef functions downstream of Atoh1 and Gfi1 in the pathway of intestinal secretory cell specification and differentiation.

SPDEF is required for activation of goblet cell genes in LS174T human colon cancer cells

Notch/γ-secretase inhibitors (GSIs) activate expression of goblet cell genes (*AGR2* [33], *MUC2* [34], *RETLNB* [35], *SPINK4* [36]), as well as *SPDEF*, in LS174T cells (Noah, Kazanjian, and Shroyer, unpublished results). To determine the requirement of SPDEF for GSI-induced goblet cell gene activation, we utilized RNA interference to reduce SPDEF expression in LS174T cells. Two lentiviral vectors encoding distinct SPDEF-specific shRNAs were transduced into LS174T cells, and significantly reduced SPDEF protein and mRNA compared to a nontargeting shRNA control vector (Figure 3A, B). We treated SPDEF-shRNA or nontargeting-shRNA transduced LS174T cells with GSI or vehicle, and quantified gene expression by RT-qPCR. As expected, *SPDEF*, *AGR2*, *MUC2*, *RETNLB*, and *SPINK4* expression was increased upon GSI treatment of nontargeting-shRNA transduced LS174T cells (Figure 3B-F, white bars). In contrast, GSI-induced expression of all four goblet cell genes was significantly reduced in SPDEF-specific shRNA transduced cells (Figure 3C-F, shaded bars). These data show that SPDEF is required for activation of goblet cell associated genes.

Intestine-specific inducible Spdef expression in *Spdef*$^{dox\text{-}intestine}$ mice

To determine the role of Spdef in intestinal epithelial differentiation *in vivo*, animals that express Spdef in a spatially and temporally restricted manner were generated. *Fabpl*$^{4x\ at\ -132}$*Cre* (that express Cre in a mosaic pattern in the epithelium of distal ileum and colon [31,37]), *Gt(ROSA)26Sor*$^{tm1(rtTA,EGFP)Nagy}$ (that express the *reverse tetracycline transactivator*, *rtTA*, and *enhanced green fluorescent protein*, *EGFP*, genes upon Cre mediated recombination [30]), and *TRE2-Spdef* (that express Spdef upon tetracycline activation of rtTA [29]) strains were intercrossed to produce tritransgenic [*Fabpl*$^{4x\ at\ -132}$*Cre*; *Gt(ROSA)26Sor*$^{tm1(rtTA,EGFP)Nagy}$; *TRE2-Spdef*] mice, herein called *Spdef*$^{dox\text{-}intestine}$ mice (Figure 4A). In *Spdef*$^{dox\text{-}intestine}$ mice, EGFP marks crypts that have undergone cre-mediated recombination and therefore can activate Spdef upon DOX treatment. As shown in Figure 4B-C, we observed patchy expression of GFP resulting from the crypt-by-crypt mosaic expression of Cre in *Spdef*$^{dox\text{-}intestine}$ mice. After two days of DOX treatment, *Spdef*$^{dox\text{-}intestine}$ mice showed robust expression of Spdef in recombined crypts (Figure 4D-G). Thus, *Spdef*$^{dox\text{-}intestine}$ mice show intestine-specific inducible expression of Spdef.

NIH-PA Author Manuscript

NIH-PA Author Manuscript

NIH-PA Author Manuscript

Spdef increases goblet cells at the expense of other epithelial cell types

Spdef$^{dox\text{-}intestine}$ and bitransgenic [*Fabpl*$^{4x\ at\ -132}$*Cre*; *Gt(ROSA)26Sor*$^{tm1(rtTA,EGFP)Nagy}$] control littermates, herein referred to as *Spdef*^{WT}, were treated with DOX for up to two months. After 2 days of DOX treatment, there were no differences in crypt/villus architecture or epithelial differentiation between *Spdef*$^{dox\text{-}intestine}$ and *Spdef*^{WT} mice (Figure 5A, B). In contrast, after 2 months of DOX, Spdef-expressing epithelium showed increased staining by periodic acid Schiff/Alcian blue (PAS/AB), with some crypts almost completely converted to PAS/AB-positive cells (Figure 5D). We confirmed that these were mucin-positive goblet cells by staining for Muc2, demonstrating a dramatic increase of Muc2-positive cells in Spdef-expressing epithelium (Figure 5C). To confirm the conversion of crypt progenitors to goblet cells, we performed transmission electron microscopy (TEM) of Spdef-expressing crypts in 2 month DOX treated mice. Spdef-expressing crypts were identified as PAS-positive/lysozyme-negative (see Figure 6C) in serial sections (Figure 5E); TEM showed absence of Paneth cells and nascent goblet cells throughout these crypts (Figure 5F). The increase in goblet cells was further demonstrated by performing immunoblot for the secreted goblet cell protein Relm-β, which was increased in intestinal tissues from *Spdef*$^{dox\text{-}intestine}$ mice at all time points following DOX treatment (Supplemental Figure 2B). Next, we stained tissues with UEA1, a lectin that binds mucin glycoproteins in goblet and Paneth cell secretory granules, and the glycocalyx overlying the brush border of absorptive enterocytes. Increased UEA1 staining of goblet cells and along the brush border was observed in Spdef-expressing epithelium (Supplemental Figure 2A). Paneth cell granule UEA1 staining was lost in Spdef-expressing crypts, suggesting a negative effect of Spdef on Paneth cell maturation.

We examined differentiation of other epithelial lineages by immunohistochemistry with lineage-specific markers. As shown in Figure 6E-F, we observed a quantitative reduction in the number of chromogranin A-positive enteroendocrine cells after 2 months of DOX treatment of *Spdef*$^{dox\text{-}intestine}$ mice. This effect was seen in Spdef-expressing epithelia both in ileum (3- fold reduction; Figure 6F) and colon (6-fold reduction; Figure 6F). Lysozyme, a marker of Paneth cells, was absent in Spdef-expressing crypts, confirming the loss of mature Paneth cells seen with UEA1 (Figure 6C, D). Finally, absorptive enterocytes were stained for the brush border enzyme dipeptidyl peptidase IV (DPPIV), and with phalloidin (which stains filamentous actin in the brush border microvilli). Staining for both DPPIV and phalloidin was diminished in Spdef-expressing epithelium that displayed goblet cell hyperplasia (Figure 6A, B; Supplemental Figure 3A, B), corresponding to a reduction in the number of absorptive enterocytes. Of note, DPPIV is normally found at the brush border of intestinal enterocytes, but was detected intracellularly in Spdef-expressing enterocytes, suggesting a potential defect in membrane protein trafficking (Supplemental Figure 3C). Together, these data suggest that Spdef expression increases production of goblet cells with a corresponding reduction in other epithelial cells, particularly Paneth and enteroendocrine cells.

Spdef blocks proliferation of intestinal progenitor cells

Following 2 days of DOX, strong Spdef expression was observed in *Spdef*$^{dox\text{-}intestine}$ mice as measured by immunohistochemistry, immunoblot, and RT-qPCR (Figure 7A, E, F). However, progressive loss of Spdef expression was noted during continuous DOX treatment (Figure 7A-F). At later time points fewer Spdef-expressing crypts were found: in the ileum of DOX treated *Spdef*$^{dox\text{-}intestine}$ mice, the percentage of Spdef-expressing crypts shrank from 24% after 2 days of DOX treatment, to 14% after 6 days, and 8% after 2 months of treatment (Figure 7B). To further elucidate the mechanism of loss of Spdef expressing crypts over time, we quantified the number of EGFP expressing crypts (reflecting Cre-mediated recombination of the *Gt(ROSA)26Sor*$^{tm1(rtTA,EGFP)Nagy}$ allele) in *Spdef*$^{dox\text{-}intestine}$

NIH-PA Author Manuscript

NIH-PA Author Manuscript

NIH-PA Author Manuscript

and *Spdef*^{WT} mice following 2 days and 2 months of DOX treatment (Figure 7C). We found that EGFP expression was lost along with Spdef expression: after two days on DOX, ~20% of ileal crypts expressed EGFP in both *Spdef*$^{dox\text{-}intestine}$ and *Spdef*^{WT} mice; in contrast, after two months on DOX, *Spdef*^{WT} mice had maintained ~20% of crypts expressing EGFP, whereas EGFP expression fell to ~8% of ileal crypts in *Spdef*$^{dox\text{-}intestine}$ mice (Figure 7D). This pattern of loss of EGFP expressing crypts matched that of progressive loss of Spdef expressing crypts.

To determine the basis for progressive loss of transgenic Spdef expression, we examined the effect of Spdef on proliferation of crypt progenitors. Following two days of DOX treatment of *Spdef*$^{dox\text{-}intestine}$ mice, we observed a dramatic reduction in proliferation in crypts expressing high levels of Spdef, as measured by BrdU incorporation (Figure 8A-C). This Spdef-mediated reduction in proliferation was more pronounced in the colon than in the ileum (7.5-fold reduction in colonic proliferation versus 2.5-fold reduction in ileum; Figure 8C). This effect was also seen in mice treated with DOX for 6 days or 2 months (data not shown). Another potential explanation for their progressive loss is death of Spdef-expressing cells. However, Spdef-expressing cells showed no increase in apoptosis at any time, as measured by morphologic changes or cleaved caspase-3 immunohistochemistry (Figure 8D-G).

We further investigated the effect of Spdef expression by generating *Spdef*$^{dox\text{-}intestine}$ mice using the pan-intestinal *Villin-cre* transgene [38] rather than the mosaic *Fabpl*$^{4x\ at\ -132}$*Cre*. When treated with DOX for 2 days, [*Villincre; Spdef*$^{dox\text{-}intestine}$] mice showed robust Spdef expression throughout the entire intestinal epithelium (Supplementary Figure 4C). In agreement with our previous experiment (Figure 8), Spdef expression dramatically reduced proliferation within the crypt progenitors in DOX treated [*Villin-cre; Spdef*$^{dox\text{-}intestine}$] mice (Supplementary Figure 4A-B) without inducing apoptosis (Supplementary Figure 4D). The proliferative arrest directed by Spdef was so profound that by 6 days of DOX treatment, all mice had to be euthanized due to acute morbidity including weight loss, diarrhea, and appearance of rectal blood. Together, these data show that Spdef blocks proliferation of intestinal progenitors, and that Spdef-expressing crypts are at a selective disadvantage compared to adjacent non-expressing crypts, resulting in progressive loss of Spdef-expressing crypts.

Discussion

In this study, we have identified the ETS-domain transcription factor Spdef as a new regulator of intestinal differentiation and homeostasis. Spdef expression in the intestinal epithelium is dependent on Atoh1 and Gfi1, transcription factors that function within intestinal progenitors to regulate cell fate decisions [4,8,32] (Figure 2). Using the tetracycline inducible system to express Spdef in the intestinal epithelium of adult mice, we found that Spdef was sufficient to promote goblet cell differentiation at the expense of other epithelial cell types (Figures 5-6) and to cause profound cell cycle arrest of intestinal progenitors (Figure 8) that is lethal if it is maintained throughout the intestinal epithelium (Supplemental Figure 4). Spdef also was necessary for GSI-induced activation goblet cell associated genes in LS174T colon cancer cells (Figure 3). Together, these results suggest that Spdef functions to regulate terminal differentiation of intestinal goblet cells.

Spdef expression increased goblet cell numbers and decreased enteroendocrine, Paneth, and absorptive enterocytes. This was most dramatic for Paneth cells, which were absent in Spdef-expressing crypts (Figure 5-6). Enteroendocrine cells were reduced by 3-6 fold in Spdef-expressing epithelia (Figure 6). Absorptive enterocytes were intermittently reduced, with some Spdef-expressing crypts showing conversion of all progenitors into goblet cells

NIH-PA Author Manuscript

NIH-PA Author Manuscript

NIH-PA Author Manuscript

(Figure 5D). We relate this differential conversion of intestinal epithelial cells to their ontogenic relationship to goblet cells: Paneth cells, which occasionally express Spdef (Figure 1) and which we hypothesize derive from a goblet/Paneth progenitor [8], are most easily converted to goblet cells by Spdef; whereas enteroendocrine cells, which share a common Atoh1-positive secretory progenitor with goblet cells [4], are moderately convertible to goblet cells. Absorptive enterocytes share only multipotent progenitors (stem cells) with goblet cells and are therefore least convertible into goblet cells by Spdef. The concept that Spdef infrequently converts stem cells into terminally differentiated goblet cells is further supported by the progressive depletion of Spdef-expressing crypts during prolonged DOX administration (Figure 7).

We observed profound cell cycle inhibition and progressive depletion of Spdef-expressing crypts (Figure 8). We also found that expression of Spdef throughout the entire intestinal epithelium is lethal. Together, these data suggest that Spdef expression depletes crypts of self-renewing progenitors (stem cells), and therefore Spdef-expressing crypts are at a selective disadvantage compared to non-expressing crypts.

Recently, we showed that Spdef regulates pulmonary goblet cell hyperplasia in response to allergen and IL-13 in a STAT-6 dependent manner [29]. Together, our results suggest that Spdef may be a key regulator of the mucinous cell phenotype in other epithelia. Our data in LS174T cells suggests that intestinal Spdef expression is under control of the Notch pathway (Figure 3). It will be interesting to determine if IL-13 or other T-helper type 2 stimuli induce Spdef in the intestine, and whether this is a STAT-6 and/or Notch dependent response.

Spdef has been previously studied in prostate and breast cancers, where its protein expression was decreased in more invasive tumors [26,28,39,40]. In breast and prostate cancers, Spdef may function as a tumor suppressor by inhibiting invasion and metastasis [41,42] and/or tumor growth and survival [28,43]. Here, we show that Spdef inhibits proliferation of intestinal progenitors (Figure 8). We suggest that Spdef might have similar activity in intestinal tumor cells, where it may be a key mediator of Atoh1's tumor suppressive activity [44]. It will be interesting to determine if Spdef is sufficient to activate goblet cell differentiation and block proliferation in Atoh1-mutant tissues, and to determine the role of Spdef in colon cancer.

Supplementary Material

Refer to Web version on PubMed Central for supplementary material.

Acknowledgments

We thank Gang Chen for advice and for sharing unpublished observations. We thank Jefferson Vallance and Tasneem Kaleem for excellent technical assistance. We thank Dr. Gary Wu for the Relm-β antibody. Additional antibodies were obtained from the Developmental Studies Hybridoma Bank. This study was supported by NIH/NIDDK grants DK071686, DK084167, and DK078392, NIH/NHLBI grants HL095580 and HL090156, and an American Gastroenterology Association/FDHN Research Scholars Award.

Grant Support: NIH K01 DK071686, NIH P30 DK078392, AGA/FDHN Research Scholars Award.

Abbreviations

SPDEF	SAM pointed domain ETS factor
BrdU	bromodeoxyuridine
OCT	optimum cutting temperature embedding medium

NIH-PA Author Manuscript

NIH-PA Author Manuscript

NIH-PA Author Manuscript

PBS	phosphate buffered saline
PFA	paraformaldehyde
DOX	doxycycline
UEA1	*Ulex europaeus* agluttinin 1

References

1. Fre S, Huyghe M, Mourikis P, Robine S, Louvard D, Artavanis-Tsakonas S. Notch signals control the fate of immature progenitor cells in the intestine. Nature 2005;435:964–968. [PubMed: 15959516]
2. Stanger BZ, Datar R, Murtaugh LC, Melton DA. Direct regulation of intestinal fate by Notch. Proc Natl Acad Sci U S A 2005;102:12443–12448. [PubMed: 16107537]
3. van Es JH, van Gijn ME, Riccio O, van den Born M, Vooijs M, Begthel H, Cozijnsen M, Robine S, Winton DJ, Radtke F, Clevers H. Notch/gamma-secretase inhibition turns proliferative cells in intestinal crypts and adenomas into goblet cells. Nature 2005;435:959–963. [PubMed: 15959515]
4. Yang Q, Bermingham NA, Finegold MJ, Zoghbi HY. Requirement of Math1 for secretory cell lineage commitment in the mouse intestine. Science 2001;294:2155–2158. [PubMed: 11739954]
5. Lee CS, Perreault N, Brestelli JE, Kaestner KH. Neurogenin 3 is essential for the proper specification of gastric enteroendocrine cells and the maintenance of gastric epithelial cell identity. Genes Dev 2002;16:1488–1497. [PubMed: 12080087]
6. Schonhoff SE, Giel-Moloney M, Leiter AB. Neurogenin 3-expressing progenitor cells in the gastrointestinal tract differentiate into both endocrine and non-endocrine cell types. Dev Biol 2004;270:443–454. [PubMed: 15183725]
7. Lopez-Diaz L, Jain RN, Keeley TM, VanDussen KL, Brunkan CS, Gumucio DL, Samuelson LC. Intestinal Neurogenin 3 directs differentiation of a bipotential secretory progenitor to endocrine cell rather than goblet cell fate. Dev Biol 2007;309:298–305. [PubMed: 17706959]
8. Shroyer NF, Wallis D, Venken KJ, Bellen HJ, Zoghbi HY. Gfi1 functions downstream of Math1 to control intestinal secretory cell subtype allocation and differentiation. Genes Dev 2005;19:2412–2417. [PubMed: 16230531]
9. Korinek V, Barker N, Moerer P, van Donselaar E, Huls G, Peters PJ, Clevers H. Depletion of epithelial stem-cell compartments in the small intestine of mice lacking Tcf-4. Nat Genet 1998;19:379–383. [PubMed: 9697701]
10. Pinto D, Gregorieff A, Begthel H, Clevers H. Canonical Wnt signals are essential for homeostasis of the intestinal epithelium. Genes Dev 2003;17:1709–1713. [PubMed: 12865297]
11. Batlle E, Henderson JT, Beghtel H, van den Born MM, Sancho E, Huls G, Meeldijk J, Robertson J, van de Wetering M, Pawson T, Clevers H. Beta-catenin and TCF mediate cell positioning in the intestinal epithelium by controlling the expression of EphB/ephrinB. Cell 2002;111:251–263. [PubMed: 12408869]
12. van Es JH, Jay P, Gregorieff A, van Gijn ME, Jonkheer S, Hatzis P, Thiele A, van den Born M, Begthel H, Brabletz T, Taketo MM, Clevers H. Wnt signalling induces maturation of Paneth cells in intestinal crypts. Nat Cell Biol 2005;7:381–386. [PubMed: 15778706]
13. Andreu P, Colnot S, Godard C, Gad S, Chafey P, Niwa-Kawakita M, Laurent-Puig P, Kahn A, Robine S, Perret C, Romagnolo B. Crypt-restricted proliferation and commitment to the Paneth cell lineage following Apc loss in the mouse intestine. Development 2005;132:1443–1451. [PubMed: 15716339]
14. Shorning BY, Zabkiewicz J, McCarthy A, Pearson HB, Winton DJ, Sansom OJ, Ashworth A, Clarke AR. Lkb1 deficiency alters goblet and paneth cell differentiation in the small intestine. PLoS ONE 2009;4:e4264. [PubMed: 19165340]
15. Simmen FA, Xiao R, Velarde MC, Nicholson RD, Bowman MT, Fujii-Kuriyama Y, Oh SP, Simmen RC. Dysregulation of intestinal crypt cell proliferation and villus cell migration in mice

NIH-PA Author Manuscript

NIH-PA Author Manuscript

NIH-PA Author Manuscript

lacking Kruppel-like factor 9. Am J Physiol Gastrointest Liver Physiol 2007;292:G1757–1769. [PubMed: 17379758]

16. Bastide P, Darido C, Pannequin J, Kist R, Robine S, Marty-Double C, Bibeau F, Scherer G, Joubert D, Hollande F, Blache P, Jay P. Sox9 regulates cell proliferation and is required for Paneth cell differentiation in the intestinal epithelium. J Cell Biol 2007;178:635–648. [PubMed: 17698607]
17. Mori-Akiyama Y, van den Born M, van Es JH, Hamilton SR, Adams HP, Zhang J, Clevers H, de Crombrugghe B. SOX9 is required for the differentiation of paneth cells in the intestinal epithelium. Gastroenterology 2007;133:539–546. [PubMed: 17681175]
18. Katz JP, Perreault N, Goldstein BG, Lee CS, Labosky PA, Yang VW, Kaestner KH. The zinc-finger transcription factor Klf4 is required for terminal differentiation of goblet cells in the colon. Development 2002;129:2619–2628. [PubMed: 12015290]
19. Ng AY, Waring P, Ristevski S, Wang C, Wilson T, Pritchard M, Hertzog P, Kola I. Inactivation of the transcription factor Elf3 in mice results in dysmorphogenesis and altered differentiation of intestinal epithelium. Gastroenterology 2002;122:1455–1466. [PubMed: 11984530]
20. Shroyer NF, Norris J, Kazanjian A, Henning SJ. Gene expression profiling of Gfi1-mutant adult intestinal crypts identifies a potential role in regulation of cell cycle within the intestine. Digestive Diseases Week. 2007
21. Oettgen P, Finger E, Sun Z, Akbarali Y, Thamrongsak U, Boltax J, Grall F, Dube A, Weiss A, Brown L, Quinn G, Kas K, Endress G, Kunsch C, Libermann TA. PDEF, a novel prostate epithelium-specific ets transcription factor, interacts with the androgen receptor and activates prostate-specific antigen gene expression. J Biol Chem 2000;275:1216–1225. [PubMed: 10625666]
22. Yamada N, Tamai Y, Miyamoto H, Nozaki M. Cloning and expression of the mouse Pse gene encoding a novel Ets family member. Gene 2000;241:267–274. [PubMed: 10675039]
23. Chen H, Nandi AK, Li X, Bieberich CJ. NKX-3.1 interacts with prostate-derived Ets factor and regulates the activity of the PSA promoter. Cancer Res 2002;62:338–340. [PubMed: 11809674]
24. Hollenhorst PC, Shah AA, Hopkins C, Graves BJ. Genome-wide analyses reveal properties of redundant and specific promoter occupancy within the ETS gene family. Genes Dev 2007;21:1882–1894. [PubMed: 17652178]
25. Wang Y, Feng L, Said M, Balderman S, Fayazi Z, Liu Y, Ghosh D, Gulick AM. Analysis of the 2.0 A crystal structure of the protein-DNA complex of the human PDEF Ets domain bound to the prostate specific antigen regulatory site. Biochemistry 2005;44:7095–7106. [PubMed: 15882048]
26. Sood AK, Saxena R, Groth J, Desouki MM, Cheewakriangkrai C, Rodabaugh KJ, Kasyapa CS, Geradts J. Expression characteristics of prostate-derived Ets factor support a role in breast and prostate cancer progression. Hum Pathol 2007;38:1628–1638. [PubMed: 17521701]
27. Turner DP, Findlay VJ, Kirven AD, Moussa O, Watson DK. Global Gene Expression Analysis Identifies PDEF Transcriptional Networks Regulating Cell Migration during Cancer Progression. Mol Biol Cell. 2008
28. Feldman RJ, Sementchenko VI, Gayed M, Fraig MM, Watson DK. Pdef expression in human breast cancer is correlated with invasive potential and altered gene expression. Cancer Res 2003;63:4626–4631. [PubMed: 12907642]
29. Park KS, Korfhagen TR, Bruno MD, Kitzmiller JA, Wan H, Wert SE, Khurana Hershey GK, Chen G, Whitsett JA. SPDEF regulates goblet cell hyperplasia in the airway epithelium. J Clin Invest 2007;117:978–988. [PubMed: 17347682]
30. Belteki G, Haigh J, Kabacs N, Haigh K, Sison K, Costantini F, Whitsett J, Quaggin SE, Nagy A. Conditional and inducible transgene expression in mice through the combinatorial use of Cre-mediated recombination and tetracycline induction. Nucleic Acids Res 2005;33:e51. [PubMed: 15784609]
31. Saam JR, Gordon JI. Inducible gene knockouts in the small intestinal and colonic epithelium. J Biol Chem 1999;274:38071–38082. [PubMed: 10608876]
32. Shroyer NF, Helmrath MA, Wang VY, Antalffy B, Henning SJ, Zoghbi HY. Intestine-Specific Ablation of Mouse atonal homolog 1 (Math1) Reveals a Role in Cellular Homeostasis. Gastroenterology 2007;132:2478–2488. [PubMed: 17570220]

NIH-PA Author Manuscript

NIH-PA Author Manuscript

NIH-PA Author Manuscript

33. Komiya T, Tanigawa Y, Hirohashi S. Cloning of the gene gob-4, which is expressed in intestinal goblet cells in mice. Biochim Biophys Acta 1999;1444:434–438. [PubMed: 10095068]
34. Gum JR, Byrd JC, Hicks JW, Toribara NW, Lamport DT, Kim YS. Molecular cloning of human intestinal mucin cDNAs. Sequence analysis and evidence for genetic polymorphism. J Biol Chem 1989;264:6480–6487. [PubMed: 2703501]
35. Steppan CM, Brown EJ, Wright CM, Bhat S, Banerjee RR, Dai CY, Enders GH, Silberg DG, Wen X, Wu GD, Lazar MA. A family of tissue-specific resistin-like molecules. Proc Natl Acad Sci U S A 2001;98:502–506. [PubMed: 11209052]
36. Metsis M, Cintra A, Solfrini V, Ernfors P, Bortolotti F, Morrasutti DG, Ostenson CG, Efendic S, Agerberth B, Mutt V, et al. Molecular cloning of PEC-60 and expression of its mRNA and peptide in the gastrointestinal tract and immune system. J Biol Chem 1992;267:19829–19832. [PubMed: 1400298]
37. Wong MH, Saam JR, Stappenbeck TS, Rexer CH, Gordon JI. Genetic mosaic analysis based on Cre recombinase and navigated laser capture microdissection. Proc Natl Acad Sci U S A 2000;97:12601–12606. [PubMed: 11050178]
38. Madison BB, Dunbar L, Qiao XT, Braunstein K, Braunstein E, Gumucio DL. Cis elements of the villin gene control expression in restricted domains of the vertical (crypt) and horizontal (duodenum, cecum) axes of the intestine. J Biol Chem 2002;277:33275–33283. [PubMed: 12065599]
39. Tsujimoto Y, Nonomura N, Takayama H, Yomogida K, Nozawa M, Nishimura K, Okuyama A, Nozaki M, Aozasa K. Utility of immunohistochemical detection of prostate-specific Ets for the diagnosis of benign and malignant prostatic epithelial lesions. Int J Urol 2002;9:167–172. [PubMed: 12010329]
40. Mitas M, Mikhitarian K, Hoover L, Lockett MA, Kelley L, Hill A, Gillanders WE, Cole DJ. Prostate-Specific Ets (PSE) factor: a novel marker for detection of metastatic breast cancer in axillary lymph nodes. Br J Cancer 2002;86:899–904. [PubMed: 11953821]
41. Gu X, Zerbini LF, Otu HH, Bhasin M, Yang Q, Joseph MG, Grall F, Onatunde T, Correa RG, Libermann TA. Reduced PDEF expression increases invasion and expression of mesenchymal genes in prostate cancer cells. Cancer Res 2007;67:4219–4226. [PubMed: 17483333]
42. Turner DP, Moussa O, Sauane M, Fisher PB, Watson DK. Prostate-derived ETS factor is a mediator of metastatic potential through the inhibition of migration and invasion in breast cancer. Cancer Res 2007;67:1618–1625. [PubMed: 17308102]
43. Ghadersohi A, Pan D, Fayazi Z, Hicks DG, Winston JS, Li F. Prostate-derived Ets transcription factor (PDEF) downregulates survivin expression and inhibits breast cancer cell growth in vitro and xenograft tumor formation in vivo. Breast Cancer Res Treat 2007;102:19–30. [PubMed: 16897429]
44. Bossuyt W, Kazanjian A, De Geest N, Van Kelst S, De Hertogh G, Geboes K, Boivin GP, Luciani J, Fuks F, Chuah M, VandenDriessche T, Marynen P, Cools J, Shroyer NF, Hassan BA. Atonal homolog 1 is a tumor suppressor gene. PLoS Biol 2009;7:e39. [PubMed: 19243219]

NIH-PA Author Manuscript
NIH-PA Author Manuscript
NIH-PA Author Manuscript

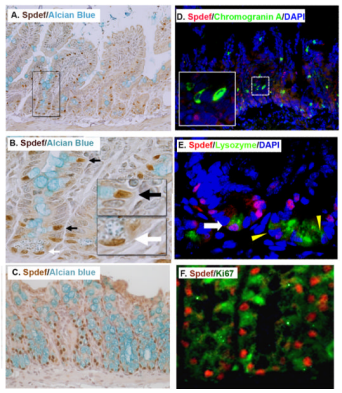

Figure 1. Spdef is expressed in intestinal goblet cells and in a subset Paneth cells

(A-C) Immunohistochemistry stained for Spdef in brown, counterstained with Alcian blue for goblet cells in (A-B) and (C) colon. (B) Higher magnification of the area boxed in (A). Black arrows show goblet cells nuclei stained with Spdef and white arrow shows Paneth cell nuclei stained with Spdef. Insets show higher magnification of boxed areas. (D) Immunofluorescence staining for Spdef (red), the enteroendocrine cell marker chromogranin A (green), and DNA stained with DAPI (blue). The inset is a higher magnification of the dotted area. No colocalization of Spdef with chromogranin A is seen. (E) Immunofluorescence staining for Spdef (red), lysozyme (green), and DAPI (blue). The white arrow shows a rare Paneth cell with Spdef staining; yellow triangles show Spdef-negative Paneth cells. (F) Immunofluorescence staining for Spdef (red) and Ki67 (green) in colon. Most Spdef positive cells do not stain with the proliferation marker Ki67.

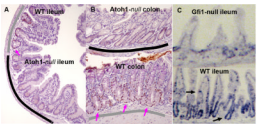

Figure 2. Protein and mRNA localization of Spdef shows loss in *Atoh1*- and *Gfi1*-null intestines

Immunohistochemical labeling of Spdef (brown) in ileum (A) and colon (B) from *Atoh1*$^{\Delta intestine}$ mice [32]. These mosaic animals contain both *wild type* (underlined in gray) and *Atoh-null* (underlined in black) crypts. Spdef is only seen in *wild type* crypts (pink arrows show nuclei stained for Spdef). (C) In situ hybridization for *Spdef* shows localization of the mRNA in crypt progenitors and goblet cells in wild type ileum (black arrows), which is largely absent from *Gfi1-null* intestine.

NIH-PA Author Manuscript
NIH-PA Author Manuscript
NIH-PA Author Manuscript

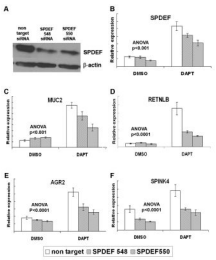

Figure 3. Inhibition of SPDEF expression in LS174T blocks activation of goblet cell associated genes

(A) SPDEF and β-actin immunoblot on protein lysate from LS174T cells transduced with lentivirus encoding SPDEF-targeted shRNAs or non-target control shRNA. (B-F) RT-qPCR analysis of LS174T cells transduced with lentivirus expressing non-targeting shRNA (white bars) or SPDEF-targeting shRNA-548 and -550 (shaded bars), then treated with DAPT or DMSO. SPDEF shRNA-548 and 550 modestly but significantly reduced SPDEF induction by DAPT, and significantly reduced *MUC2*, *SPINK4*, *AGR2*, and *RETNLB* mRNA following DAPT treatment. Y-axis shows relative expression values normalized to GAPDH. *P* values are for 2-way ANOVA for shRNA (non target vs siRNA 548 or 550) and treatment (DAPT vs. DMSO). Error bars show SEM.

NIH-PA Author Manuscript NIH-PA Author Manuscript NIH-PA Author Manuscript

NIH-PA Author Manuscript
NIH-PA Author Manuscript
NIH-PA Author Manuscript

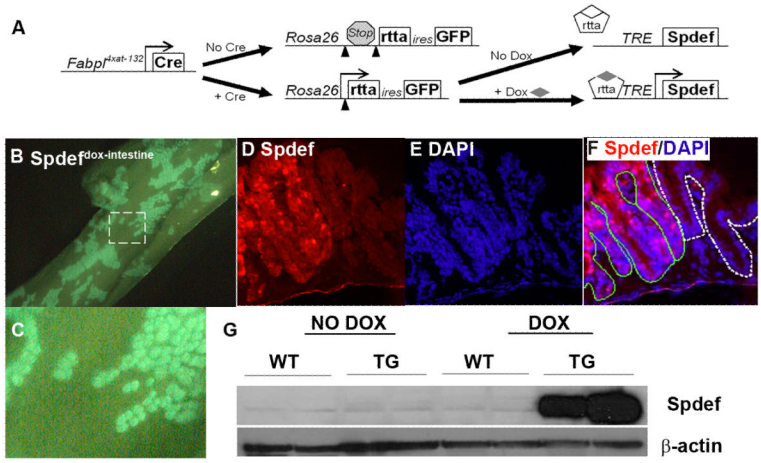

Figure 4. Doxycycline-inducible Spdef expression in *Spdef*$^{dox\text{-}intestine}$ colon

(A) Schematic of how the three alleles in *Spdef*$^{dox\text{-}intestine}$ mice cause intestine-specific, DOX-inducible expression of Spdef. (B-C) GFP fluorescence of whole colon from a *Spdef*$^{dox\text{-}intestine}$ mouse following 2 days of DOX, showing a mosaic pattern of GFP expression. (C) Close-up view of the area outlined in (B) shows the patchy crypt-by-crypt mosaic of cre-mediated recombination. (D-F) Colon section from mouse in (B), stained for Spdef (red in (D and F)) and DAPI (blue in (E and F) shows Spdef-expressing crypts (F: outlined in green) adjacent to unrecombined crypts (F: outlined in white). (G) Immunoblot of colonic tissue shows robust induction of Spdef following 2 days of DOX administration to *Spdef*$^{dox\text{-}intestine}$ (TG) but not *Spdef*^{WT} (WT) or untreated mice. Immunoblot for β-actin was used to show equivalent total protein in each lane.

NIH-PA Author Manuscript
NIH-PA Author Manuscript
NIH-PA Author Manuscript

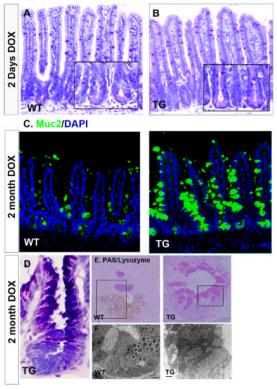

Figure 5. Spdef increases goblet cell production

Histologic analysis of DOX-treated *Spdef*^{WT} (WT) and *Spdef*$^{dox\text{-}intestine}$ (TG) mice. (A-B) Hematoxylin and periodic acid Schiff/ Alcian blue (PAS/AB) stained ileum shows no overt differences between (A) WT and (B) TG after 2 days of DOX. Insets show high power image of crypts. (C) Immunofluorescence images of ileum from WT and TG after 2 months of DOX. Muc2 staining (green) for goblet cells is increased in TG ileum. (D) High power image of a crypt stained with PAS/AB shows only goblet cells in a TG mouse after 2 months of DOX. (E) Plastic embedded ileum stained for lysozyme and PAS. Lack of lysozyme staining combined with an increased PAS staining identified Spdef-expressing crypts (see Figure 6). (F) Transmission electron microscopy analysis of the serial sections of the area enclosed with black rectangles in (E) (scale bar: 2 micron). Loss of lysozyme staining along with the loss of electron dense secretory granules indicates a loss of Paneth cells in TG crypts. TG crypts are instead occupied by goblet cells with electron lucent mucin granules.

NIH-PA Author Manuscript
NIH-PA Author Manuscript
NIH-PA Author Manuscript

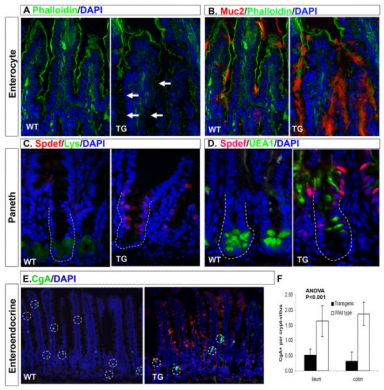

Figure 6. Spdef expression decreases absorptive, Paneth, and enteroendocrine cell numbers

Immunofluorescence analysis of ileum from *Spdef*^{WT} (WT) and *Spdef*$^{dox\text{-}intestine}$ mice (TG) treated for 2 months with DOX. DAPI staining is shown in blue and Spdef staining is shown in red except for (B) where Muc2 staining is shown in red. Green staining shows phalloidin (A, B), lysozyme (C), UEA1 (D), or chromogranin A (E). White arrows in (A) show gaps in phalloidin staining where Muc2 staining is increased (B). Dotted lines in (C,D) outline crypts. (E) Chromogranin A positive cells are circled with dotted lines. (F) Quantitation of chromogranin A positive cells in *Spdef*^{WT} and *Spdef*$^{dox\text{-}intestine}$ ileum. Error bars show SEM. Intestinal epithelia that express Spdef show decreased staining with phalloidin, chromogranin A, lysozyme, and Paneth cell-specific UEA1, and increased staining with Muc2, suggesting re-specification of cell lineages due to Spdef expression.

NIH-PA Author Manuscript
NIH-PA Author Manuscript
NIH-PA Author Manuscript

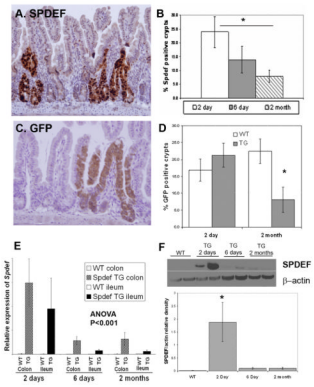

Figure 7. Progressive loss of Spdef expressing crypts during continuous transgene expression

Immunohistochemistry (in brown) for Spdef (A) and GFP (C) in mice treated with DOX for 2 days. (B&D) Quantitation of Spdef-expressing and GFP-expressing crypts at time points indicated. Both Spdef-expressing and GFP-expressing crypts decreased significantly after 2 months of DOX compared to 2 days of DOX. (E) RT-qPCR of *Spdef* expression normalized to *GAPDH* from $Spdef^{WT}$ (WT) and $Spdef^{dox\text{-}intestine}$ (TG) mice treated with DOX for up to 2 months. Duration of DOX treatment and tissue analysed are indicated on the graph. (F) Representative immunoblot for Spdef and Actin on cecal lysates from WT and TG mice treated with DOX as shown. Densitometry of band intensity for Spdef normalized to Actin is shown in the graph below. *Spdef* mRNA (E) and protein (F) levels were decreased upon continuous DOX administration to $Spdef^{dox\text{-}intestine}$ mice. * P<0.05.

NIH-PA Author Manuscript
NIH-PA Author Manuscript
NIH-PA Author Manuscript

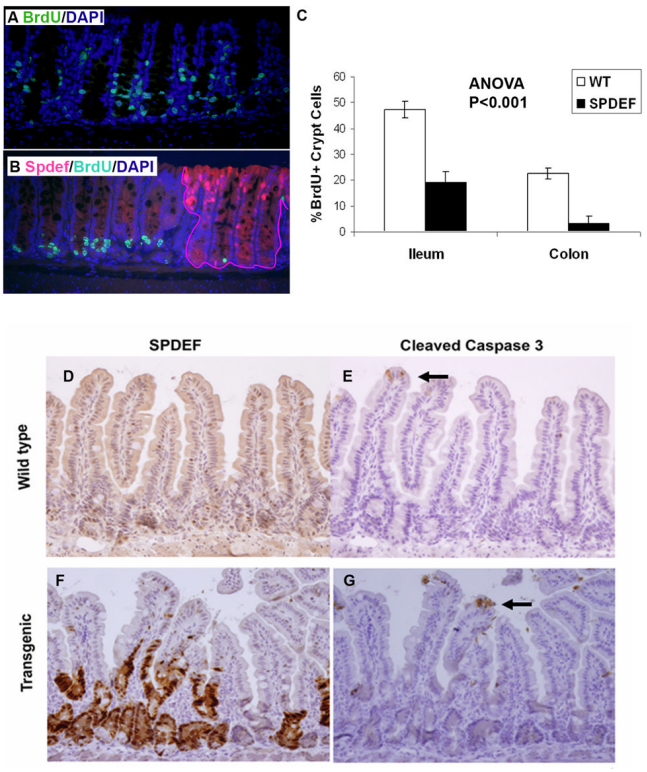

Figure 8. Spdef inhibits crypt cell proliferation

(A-B) Immunofluorescence staining for BrdU (green), Spdef (red), and DAPI (blue), is shown for *Spdef*$^{dox\text{-}intestine}$ (B) and *Spdef*^{WT} (A) mice treated with DOX for 2 days and sacrificed following a 2hr BrdU pulse. Crypts that express Spdef are outlined in (B) by the red line. (C) Quantitation of BrdU-labeled crypt cells from *Spdef*^{WT} mice (white bars) and from Spdef-expressing crypts in *Spdef*$^{dox\text{-}intestine}$ mice (black bars), showed less proliferation of Spdef-expressing crypts in both colon and ileum. (D-G) Immunohistochemistry for Spdef (D,F) and the apoptotic marker cleaved-caspase-3 (E,G) is shown in brown, counterstained with hematoxylin. Serial sections from *Spdef*$^{dox\text{-}intestine}$ (labeled as transgenic, F&G) and *Spdef*^{WT} (labeled as wild type, D&E) were used. Black arrows point to cleaved caspase 3 positive cells at the villus tip. No difference in apoptosis was observed.